Factors Controlling Adsorption Equilibria from Solution onto Solid Surfaces: The Uptake of Cinchona Alkaloids on Platinum Surfaces

ARTICLE *in* JOURNAL OF THE AMERICAN CHEMICAL SOCIETY · JANUARY 2008

Impact Factor: 12.11 · DOI: 10.1021/ja076011a · Source: PubMed

3 AUTHORS, INCLUDING:

Zhen Ma
Fudan University
98 PUBLICATIONS **2,201** CITATIONS
SEE PROFILE

Francisco Zaera
University of California, Riverside
376 PUBLICATIONS **12,219** CITATIONS
SEE PROFILE

J|A|C|S
ARTICLES
Published on Web 11/29/2007

Factors Controlling Adsorption Equilibria from Solution onto Solid Surfaces: The Uptake of Cinchona Alkaloids on Platinum Surfaces

Zhen Ma, Ilkeun Lee, and Francisco Zaera*

Contribution from the Department of Chemistry, University of California, Riverside, California 92521

Received August 9, 2007; E-mail: zaera@ucr.edu

Abstract: The room-temperature adsorption of four closely related cinchona alkaloids and three reference quinoline-based compounds from CCl_4 solutions onto a polycrystalline platinum surface was characterized by in situ reflection−absorption infrared spectroscopy (RAIRS). The adsorption equilibrium constants (K_{ads}) were found to follow the sequence cinchonine > quinidine > cinchonidine > quinine > 6-methoxyquinoline > lepidine > quinoline. Some of this ordering can be explained by differences in solubility, but quinidine displays a much larger K_{ads} than expected on the basis of its large relative solubility; bonding to the surface must also play a role in determining its behavior. It was determined that each alkaloid binds differently on Pt at saturation coverages. While the quinoline ring of cinchonidine tilts along its long axis to optimize $\pi-\pi$ intermolecular interactions, in cinchonine it tilts along the short axis and bonds through the lone electron pair of the nitrogen atom instead, and both quinine and quinidine exhibit additional bonding via the methoxy oxygen atom at intermediate concentrations. Perhaps a more surprising result from this work is the fact that cinchonine displays a higher K_{ads} than cinchonidine, quinine, or quinidine even though, according to previous work, it can be easily displaced from the surface by any of those other cinchona alkaloids. A full explanation of these observations requires consideration of the solvent above the adsorbed species.

1. Introduction

Cinchona alkaloids are promising chiral modifiers in heterogeneous catalysis.[1,2] Cinchonidine in particular has been shown to promote the selective hydrogenation of α-keto ester to one single α-hydroxo ester enantiomer with enantioselectivities in excesses of 95%.[2−5] Cinchonine, a near enantiomer of cinchonidine, promotes the production of the opposite α-hydroxo ester enantiomer but without the same effectiveness,[6,7] and similar enantioselectivity differences have been reported with other pairs of near enantiomers.[8−12] In fact, when mixtures of several cinchona alkaloids are used in this catalysis, nonlinear effects are observed where one of the compounds controls the overall chiral modification.[8,10,12−14] This has been explained by the preferential adsorption of that cinchona on the surface.[11,15,16]

These observations raise interesting questions regarding the factors that control relative adsorption strengths among seemingly similar molecules. In order to explore this issue, we have performed an in situ characterization of the adsorption of a family of related cinchona alkaloids on platinum surfaces using reflection−absorption infrared spectroscopy (RAIRS). Some common adsorption behavior was observed, but characteristics unique to each compound were also identified. Specifically, all the alkaloids appear to bond to the surface via the quinoline ring and to change their adsorption geometry as a function of concentration in solution, from flat binding to a more tilted configuration. However, while the quinoline ring in cinchonidine tilts mostly along its long axis, in cinchonine it tilts along the short axis instead, and develops a stronger interaction between the quinoline nitrogen atom and the surface. Furthermore, both quinine and quinidine adopt a third bonding mode involving the oxygen atom of the methoxy group at intermediate coverages. These differences in bonding, together with variations in solubilities, are sufficient to justify most of the behavior observed in competitive adsorption environments and in catalysis.

2. Experimental Section

The experimental setup used for the in situ infrared (IR) spectroscopy characterization of liquid−solid interfaces has been already described

(1) Orito, Y.; Imai, S.; Niwa, S.; Nguyen, G. H. *Yuki Gosei Kagaku Kyokaishi* **1979**, *37*, 173.
(2) Baiker, A. *J. Mol. Catal. A: Chem.* **1997**, *115*, 473.
(3) Wells, P. B.; Wilkinson, A. G. *Top. Catal.* **1998**, *5*, 39.
(4) LeBlond, C.; Wang, J.; Andrews, A. T.; Sun, Y.-K. *Top. Catal.* **2000**, *13*, 169.
(5) Blaser, H. U. *Catal. Today* **2000**, *60*, 161.
(6) Exner, C.; Pfaltz, A.; Studer, M.; Blaser, H.-U. *Adv. Synth. Catal.* **2003**, *345*, 1253.
(7) Bonalumi, N.; Vargas, A.; Ferri, D.; Bürgi, T.; Mallat, T.; Baiker, A. *J. Am. Chem. Soc.* **2005**, *127*, 8467.
(8) Simons, K. E.; Meheux, P. A.; Ibbotson, A.; Wells, P. B. *Stud. Surf. Sci. Catal.* **1993**, *75*, 2317.
(9) Simons, K. E.; Ibbotson, A.; Johnston, P.; Plum, H.; Wells, P. B. *J. Catal.* **1994**, *150*, 321.
(10) Huck, W.-R.; Bürgi, T.; Mallat, T.; Baiker, A. *J. Catal.* **2003**, *216*, 276.
(11) Meier, D. M.; Mallat, T.; Ferri, D.; Baiker, A. *J. Catal.* **2006**, *244*, 260.
(12) Meier, D. M.; Ferri, D.; Mallat, T.; Baiker, A. *J. Catal.* **2007**, *248*, 68.
(13) Diezi, S.; Mallat, T.; Szabo, A.; Baiker, A. *J. Catal.* **2004**, *228*, 162.
(14) Balazs, L.; Mallat, T.; Baiker, A. *J. Catal.* **2005**, *233*, 327.
(15) Baiker, A. *Catal. Today* **2005**, *100*, 159.
(16) Ma, Z.; Zaera, F. *J. Am. Chem. Soc.* **2006**, *128*, 16414.

in detail in previous publications.[17−19] Briefly, a polished polycrystalline Pt disk, 10 mm in diameter and 1 mm in thickness, is mounted on a polytetrafluoroethylene supporting rod and inserted in the center of an infrared cell sealed in its front by a transparent CaF_2 prism cut in a trapezoidal shape with two faces beveled at 60°. A micrometer is attached to the end of the sample rod to control the distance between the Pt sample and the prism, and is used to retract the surface during cleaning and exposure to the solutions and to press it against the prism for the infrared measurements. The IR beam from a Mattson Sirius 100 Fourier-transform infrared spectrometer is guided through a linear polarizer and focused through the CaF_2 prism onto the Pt disk, and the reflected light is collected and refocused into a mercury−cadmium−telluride (MCT) detector.

The general procedure followed in all experiments was as follows: the Pt disk was cleaned before each experiment by electrochemical oxidation−reduction cycles in 0.1 M $KClO_4$ for 1 h. The electrolyte was then flushed using pure CCl_4, the Pt disk pressed tightly against the prism to form a thin liquid film, and two reference IR spectra recorded, with p- and s-polarized light, respectively. Next, the solid was pulled back, the CCl_4 solvent displaced by a solution of the compound of interest, and H_2 bubbled through the liquid for 30 min to reduce the metal surface.[20] Afterward, the Pt disk was again pressed against the prism, and new p- and s-polarized spectra were recorded. The data reported here correspond to the ratio of the p/s trace ratios obtained with the solution of interest against the equivalent background p/s data obtained with the pure CCl_4 solvent. All the reported spectra correspond to averages from 512 scans, taken with 4 cm^{-1} resolution.

The following chemicals were used in this study: quinoline (Aldrich, 98%), lepidine (4-methylquinoline, Aldrich, 99%), 6-methoxyquinoline (Aldrich, 98%), cinchonine (Alfa Aesar, 98%), cinchonidine (Aldrich, 96%), quinidine (Acros, 95%), quinine (Acros, 99%), carbon tetrachloride (Aldrich, 99.9%), and H_2 (Liquid Carbonic, 99.999%). All the experiments were carried out at ambient temperature (295 ± 2 K).

3. Results

A total of seven quinoline-derived compounds were used in these studies, four related cinchona alkaloids (cinchonidine, CD, cinchonine, CN, quinine, QN, and quinidine, QD), and three reference compounds (quinoline, Q, lepidine, L, and 6-methoxyquinoline, 6-MeOQ). The molecular structures of all seven compounds are provided in Figure 1. All these chemicals bear the same quinoline ring believed to help anchor the chiral modifiers to the catalytic active metal surfaces,[15,21−23] and lepidine, cinchonine, and cinchonidine have substituent groups at the C4′ position of the quinoline ring, 6-methoxyquinoline has a methoxy group at the C6′ position, and quinine and quinidine have substituent groups at both C4′ and C6′ positions.

Figure 2 displays typical RAIRS traces for lepidine obtained under different conditions to illustrate the importance of performing the spectroscopic characterization of the adsorbed cinchona alkaloids in situ at the liquid−solid interfaces. Note here the fact that similar spectra are seen for the neat lepidine liquid, a lepidine solution in CCl_4, and lepidine adsorbed on a Pt(111) single crystal under ultrahigh vacuum (UHV) conditions. In contrast, the infrared data for lepidine adsorbed on Pt from a CCl_4 solution are quite different. Notice, for instance, the blue-

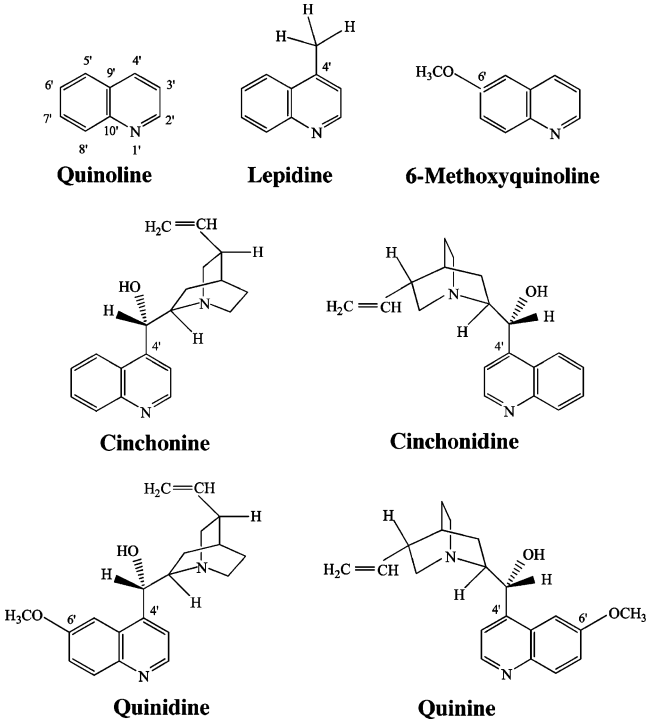

Figure 1. Molecular structures of the seven compounds used in this study: quinoline, lepidine, 6-methoxyquinoline, cinchonine, cinchonidine, quinidine, and quinine. This collection includes three reference quinoline-based compounds and four cinchona alkaloids used in catalytic chiral promotion. Note that cinchonidine and cinchonine are near enantiomers, with reverse chirality around the central alcohol and quinuclidine chiral carbon atoms, and that quinine and quinidine are identical to cinchonidine and cinchonine, respectively, except for the additional methoxy group in the C6′ position of the quinoline ring.

shift of the main quinoline ring stretching mode peak, from 1595 cm^{-1} in pure lepidine to 1604 cm^{-1} once it adsorbs on the Pt surface. Conversely, the peak at 1570 cm^{-1} red-shifts to 1548 cm^{-1}, and that at 1508 cm^{-1} decreases significantly in intensity. The data in Figure 2 show that these differences are the result of the combined effects of the bonding of the quinoline ring to the metal surface and the presence of the carbon tetrachloride solvent; no equivalent changes are seen if only one of those factors is taken into account.

RAIRS traces obtained for all seven quinoline derivatives adsorbed onto platinum surfaces from CCl_4 solutions are shown in Figure 3, and the corresponding peak assignments, made with the aid of reported data for quinoline,[24−27] monosubstituted quinoline,[28,29] cinchonidine,[30−33] cinchonine,[34] and quinine,[35] as well as quantum mechanical calculations carried out in our own laboratory, are reported in Table 1. Notice that most of the peaks in the infrared spectral window reported here correspond to in-

(17) Zaera, F. *Int. Rev. Phys. Chem.* **2002**, *21*, 433.
(18) Kubota, J.; Ma, Z.; Zaera, F. *Langmuir* **2003**, *19*, 3371.
(19) Ma, Z.; Zaera, F. *Catal. Lett.* **2004**, *96*, 5.
(20) Ma, Z.; Kubota, J.; Zaera, F. *J. Catal.* **2003**, *219*, 404.
(21) Wells, P. B.; Simons, K. E.; Slipszenko, J. A.; Griffiths, S. P.; Ewing, D. F. *J. Mol. Catal. A: Chem.* **1999**, *146*, 159.
(22) Studer, M.; Blaser, H. U.; Exner, C. *Adv. Synth. Catal.* **2003**, *345*, 45.
(23) Murzin, D.; Mäki-Arvela, P.; Toukoniitty, E.; Salmi, T. *Catal. Rev.* **2005**, *47*, 175.
(24) Chiorboli, P.; Bertoluzza, A. *Ann. Chim.* **1959**, *49*, 245.
(25) Wait, S. C., Jr.; McNerney, J. C. *J. Mol. Spectrosc.* **1970**, *34*, 56.
(26) Bandyopadhyay, I.; Manogaran, S. *Indian J. Chem., Sect. A* **2000**, *39*, 189.
(27) Özel, A. E.; Büyükmurat, Y.; Akyüz, S. *J. Mol. Struct.* **2001**, *565/566*, 455.
(28) Katritzky, A. R.; Jones, R. A. *J. Chem. Soc.* **1960**, 2942.
(29) Ozel, A. E.; Kecel, S.; Akyuz, S. *Vib. Spectrosc.* **2006**, *42*, 325.
(30) Chu, W.; LeBlanc, R. J.; Williams, C. T.; Kubota, J.; Zaera, F. *J. Phys. Chem. B* **2003**, *107*, 14365.
(31) Ferri, D.; Bürgi, T. *J. Am. Chem. Soc.* **2001**, *123*, 12074.
(32) Ma, Z.; Lee, I.; Kubota, J.; Zaera, F. *J. Mol. Catal. A: Chem.* **2004**, *216*, 199.
(33) Kraynov, A.; Suchopar, A.; D'Souza, L.; Richards, R. *Phys. Chem. Chem. Phys.* **2006**, *8*, 1321.
(34) Weselucha-Birczynska, A.; Ciechanowicz-Rutkowska, M. *J. Mol. Struct.* **2000**, *555*, 391.
(35) Frosch, T.; Schmitt, M.; Popp, J. *J. Phys. Chem. B* **2007**, *111*, 4171

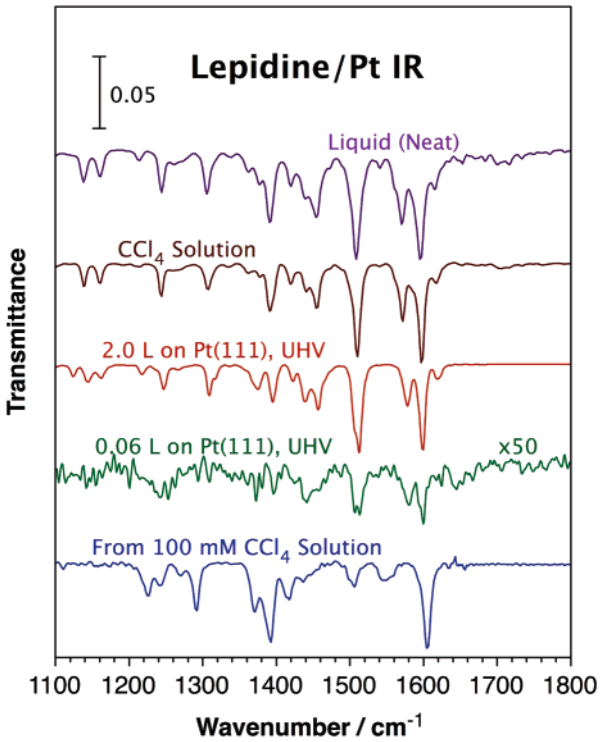

Figure 2. Infrared absorption spectra for lepidine pure, in a 100 mM CCl_4 solution, adsorbed on a Pt(111) surface under ultrahigh vacuum (UHV) conditions (for two doses, 0.06 and 2.0 L, corresponding to submonolayer and multilayer coverages), and adsorbed on a platinum polycrystalline surface from a 100 mM CCl_4 solution. Only the spectrum for the species adsorbed from solution is significantly different, indicating that it is the combined effect of surface bonding and the presence of the solvent that induces noticeable changes in the nature of the adsorbate.

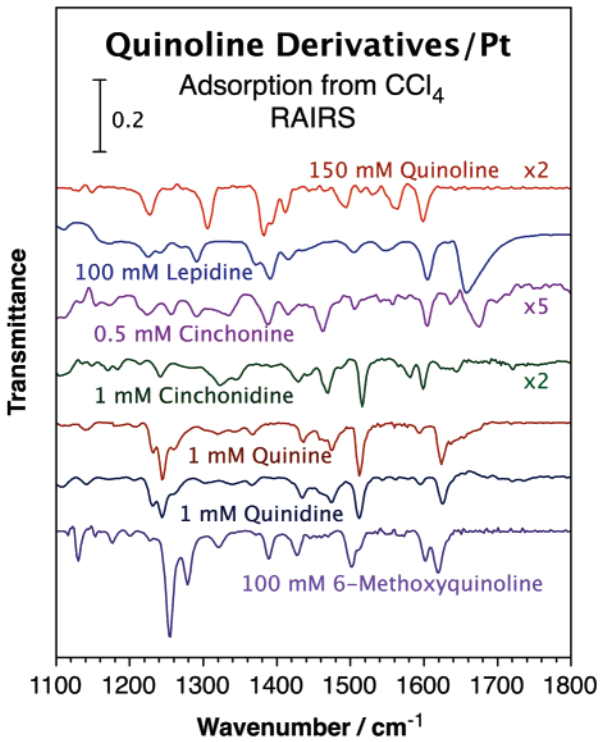

Figure 3. In situ reflection−absorption infrared spectroscopy (RAIRS) traces for quinoline, lepidine, cinchonine, cinchonidine, quinine, quinidine, and 6-methoxyquinoline adsorbed onto a Pt surface from CCl_4 solutions. Peak assignments are provided in Table 1.

plane stretchings or deformations of the quinoline ring, with a few notable exceptions (including vibrations in the methoxy group of 6-methoxyquinoline, quinine, and quinidine).

The uptake of the quinoline derivatives in Figure 1 was studied individually as a function of their concentration in the carbon tetrachloride solutions. The RAIRS data for the case of quinoline are shown in Figure 4 to illustrate some of the general trends observed. First, the peak positions in the infrared spectra are almost all invariant as a function of concentration, with the exception of a few features in the cases of quinine and quinidine (as discussed later). Second, no visible infrared absorption features are detected below a given threshold concentration, but above that the uptake is rapid and reaches saturation at specific higher concentrations. Third, in the case of the cinchona alkaloids, a significant switch in the overall appearance of the spectra is observed at intermediate concentrations due to change in adsorption geometry, from flat coordination of the aromatic ring to the surface at low coverages to a more tilted configuration at saturation.[30−32,36−39]

The latter behavior, the change in adsorption geometry with coverage, is quite common with aromatic compounds on metal surfaces[40−42] but, surprisingly, does not seem to apply to the uptake of quinoline, lepidine, or 6-methoxyquinoline. In RAIRS experiments such as ours adsorption geometries are estimated by the relative intensities of the different absorption peaks, because a surface selection rule in RAIRS with metals states that only the perpendicular dynamic dipoles of the vibrational modes contribute to the spectra.[43−46] In this case, the detection of any peaks due to in-plane quinoline ring stretching or deformation modes or C−H stretching vibrations is indicative of adsorption with the plane of the quinoline ring at an angle from the metal surface. As shown in Figure 4, for quinoline this is the case for concentrations above 2 mM. On the other hand, because of the absence of available ring out-of-plane vibrational modes in our data, it is difficult to establish if quinoline, lepidine, or 6-methoxyquinoline adopt other adsorption configurations at lower concentrations. The one point that can be made with some certainty here is that, if a flat-lying adsorption state were to exist at low concentrations for the case of 6-methoxyquinoline, the methyl asymmetric deformation mode at 1474 cm^{-1} would be expected to be visible in the RAIRS spectra, and that is not the case (see Supporting Information).

The RAIRS data for the uptake of the four cinchonas studied in this work are reported in Figures 5 and 6. In terms of the adsorption of cinchonidine and cinchonine, the predominance of peaks around 1220 and 1385 cm^{-1} due to out-of-plane deformations of the quinuclidine ring points to a flat adsorption

(36) Bürgi, T.; Zhou, Z.; Kunzle, N.; Mallat, T.; Baiker, A. *J. Catal.* **1999**, *183*, 405.
(37) Kubota, J.; Zaera, F. *J. Am. Chem. Soc.* **2001**, *123*, 11115.
(38) Chu, W.; LeBlanc, R. J.; Williams, C. T. *Catal. Commun.* **2002**, *3*, 547.
(39) Vayner, G.; Houk, K. N.; Sun, Y.-K. *J. Am. Chem. Soc.* **2004**, *126*, 199.
(40) Zaera, F. *Chem. Rev.* **1995**, *95*, 2651.
(41) Ma, Z.; Zaera, F. *Surf. Sci. Rep.* **2006**, *61*, 229.
(42) Netzer, F. P.; Ramsey, M. G. *Crit. Rev. Solid State Mater. Sci.* **1992**, *17*, 397.
(43) Greenler, R. G. *J. Chem. Phys.* **1966**, *44*, 310.
(44) Chabal, Y. J. *Surf. Sci. Rep.* **1988**, *8*, 211.
(45) Zaera, F.; Hoffmann, H.; Griffiths, P. R. *J. Electron Spectrosc. Relat. Phenom.* **1990**, *54/55*, 705.
(46) Zaera, F. Surface Structural Determinations: Optical Methods. In *Encyclopedia of Chemical Physics and Physical Chemistry*; Moore, J. H., Spencer, N. D., Eds.; IOP Publishing Inc.: Philadelphia, 2001; Vol. 2, pp 1563−1581.

Table 1. Vibrational Assignment of the Infrared Spectra of the Quinoline Derivatives Studied Here, Pure and Adsorbed on a Platinum Surface (All Frequencies Are Reported in cm^{-1})

	quinoline		lepidine		6-MeOQ		cinchonidine		cinchonine		quinine		quinidine	
assignment[a]	liquid	on Pt	liquid	on Pt	liquid	on Pt	solid	on Pt	solid	on Pt	solid	on Pt	solid	on Pt
ν_{ip}(Q ring); ν(C═C, vinyl)	1620		1613		1622	1619	1634		1638		1622	1624	1620	1626
ν_{ip}(Q ring), short axis	1595	1599	1595	1604	1595	1601	1589	1598	1591	1604	1589	1593	1587	1594
ν_{ip}(Q ring), short axis	1570	1564	1570	1548	1572		1568	1581	1568	1558			1564	1562
ν_{ip}(Q ring), long axis	1501	1492	1508	1507	1501	1502	1506	1516	1506	1505	1508	1512	1508	1512
$\delta_{as}(CH_3$, methoxy)					1474						1470	1475	1463	1474
$\gamma_{oop}(CH_2$ in QN)							1450	1469	1452	1462	1447	1458	1452	1459
δ_{ip}(C−H, Q ring)	1431	1414	1439	1417	1433	1428	1422	1430	1418	1414	1429	1437		1434
δ_{ip}(Q ring)	1392	1394	1391	1392	1377	1373	1377	-	1383	1388	1382	1369	1385	1367
ν_{ip}(Q ring)	1371	1382	1375	1370	1362		1352	1346	1356	1335	1368	1344	1358	1339
δ_{ip}(C−H, Q ring)	1314	1307	1306	1292	1323	1321	1325	1320	1323		1321	1320	1329	
δ(C−H, QN)							1263	1280	1257	1291	1261	1261	1261	1262
ν(C−O, methoxy)					1261	1278					1239	1243	1261	1243
ν(C−O, methoxy)					1227	1254					1227	1231	1251	1231
δ_{ip}(QP ring)	1222		1244	1242	1246	1228	1227	1242	1234	1259	1227	1231	1236	1231
$\tau(CH_2$, QN) + δ_{ip}(C−H, Q)	1215	1227	1214	1227	1196	1200	1205	1214	1206	1227	1203	1209	1201	1207
δ_{ip}(C−H, QB)							1179	1182	1168	1172	1181		1188	
δ_{ip}(Q ring) + δ_{ip}(C−H, Q)			1159	1160	1161	1177	1161	1165	1163	1154	1167		1167	
δ_{oop}(C−H, Q)	1140	1148	1138		1115	1130	1134	1135	1130	1135	1134	1142	1160	

[a] Q = quinoline; QP = pyridine moiety of quinoline ring; QB = benzene moiety of quinoline ring; QN = quinuclidine; ν = stretching; γ = scissoring; δ = deformation; τ = torsion; ip = in-plane; oop = out-of-plane; as = asymmetric.

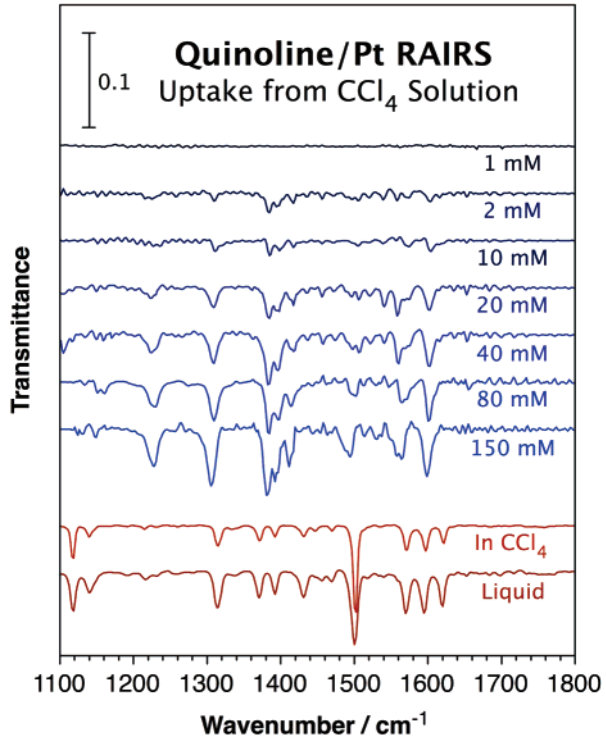

Figure 4. In situ RAIRS for quinoline adsorbed on platinum as a function of the concentration of the solution. The spectra for pure quinoline and for a 100 mM CCl_4 solution are also provided for reference. The traces for the adsorbed species are clearly different from the references, but do not change appreciably as a function of concentration other than increase in intensity because of the increases in surface coverage.

on the surface at low concentrations.[37] In fact, another feature is also clearly visible in the spectra for cinchonidine in the left panel of Figure 5 around 1470 cm^{-1} associated with out-of-plane C−H deformations in the CH_2 groups of quinuclidine. On the other hand, a new tilted adsorption geometry becomes evident at higher concentrations, starting at approximately 0.4 and 0.08 mM for cinchonidine and cinchonine respectively, as evidenced by the appearance of multiple in-plane quinoline ring stretching and deformation peaks, including the three prominent features seen between about 1500 and 1600 cm^{-1}.

The relative tilting along the short versus long axis of the quinoline ring in these adsorbates can also be determined by analyzing the relative intensities of the peaks at 1589 and 1506 cm^{-1} (for pure cinchonidine), which correspond to vibrations with dynamic dipoles oriented along each of those two axes. Hence, the relative enhancement of the signal for the vibration along the long axis (at 1516 cm^{-1}) in saturated cinchonidine layers indicates an orientation along that axis. This behavior suggests intermolecular $\pi-\pi$ stacking as the dominant force defining the adsorption geometry in this case, perhaps the same as in the solid (where chains of molecules alternate along screw axes).[47] Interestingly, cinchonine behaves quite differently; the predominance of the peak at 1604 cm^{-1} and the almost absence of any signal for the mode at 1505 cm^{-1} in the infrared spectra for high concentrations point to tilting along the short axis of the quinoline ring instead (Figure 5, right frame), and a large blue-shift of the former infrared feature, from 1591 cm^{-1} for pure cinchona to 1604 cm^{-1} once adsorbed on the platinum surface, is also apparent. The implication is that the individual molecular interaction with the surface is stronger, and may involve bonding via the lone electron pair of the nitrogen atom in the quinoline ring.

The uptake data for quinine and quinidine reported in Figure 6 points to additional idiosyncrasies in the adsorption of those cinchona alkaloids as well. In both cases the infrared spectra obtained for the saturated monolayer show only minor differences from the data for the pure or dissolved cinchona, indicating tilted adsorption but no specific ring orientation on the platinum surface (or an azimuthal angle close to the magic angle). There are also only two minor peaks visible in the spectra for low (~0.025 mM) concentrations, the 1217 and 1262 cm^{-1} features assignable to C−H deformation modes in the quinuclidine ring, suggesting an initial flat adsorption geometry like with cinchonidine and cinchonine. However, the unique behavior of both quinine and quinidine is seen at intermediate concentrations, at

(47) Oleksyn, B. J. *Acta Crystallogr., Sect. B* **1982**, *38*, 1832.

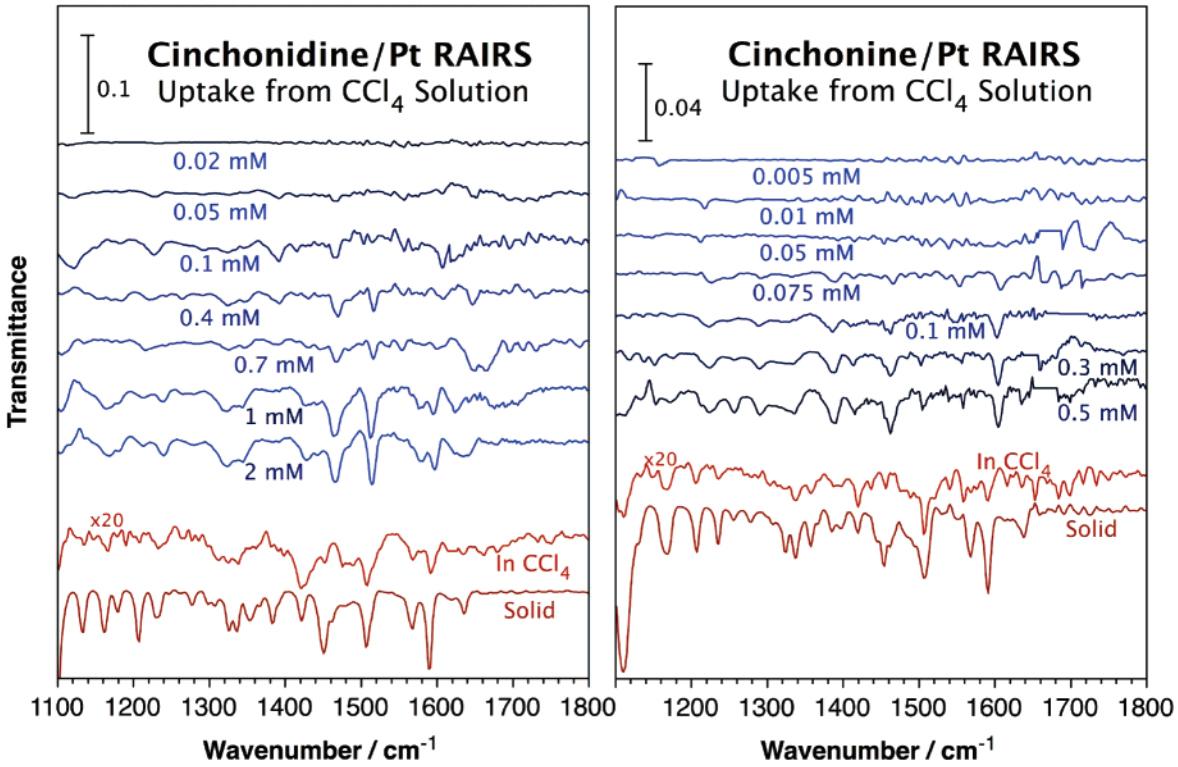

Figure 5. RAIRS for cinchonidine (left panel) and cinchonine (right panel) adsorbed on Pt as a function of solution concentration. The low-concentration data are dominated by peaks at 1220 and 1385 cm^{-1} in both cases, indicating adsorption with the quinoline ring flat on the surface. Many in-plane quinoline ring stretching and deformation peaks grow at higher concentration due to ring tilting, but significant differences are seen between cinchonidine and cinchonine due to differences in bonding to the surface. Also notice that the onset for the quinoline ring tilting occurs at significantly lower concentrations with cinchonine than with cinchonidine.

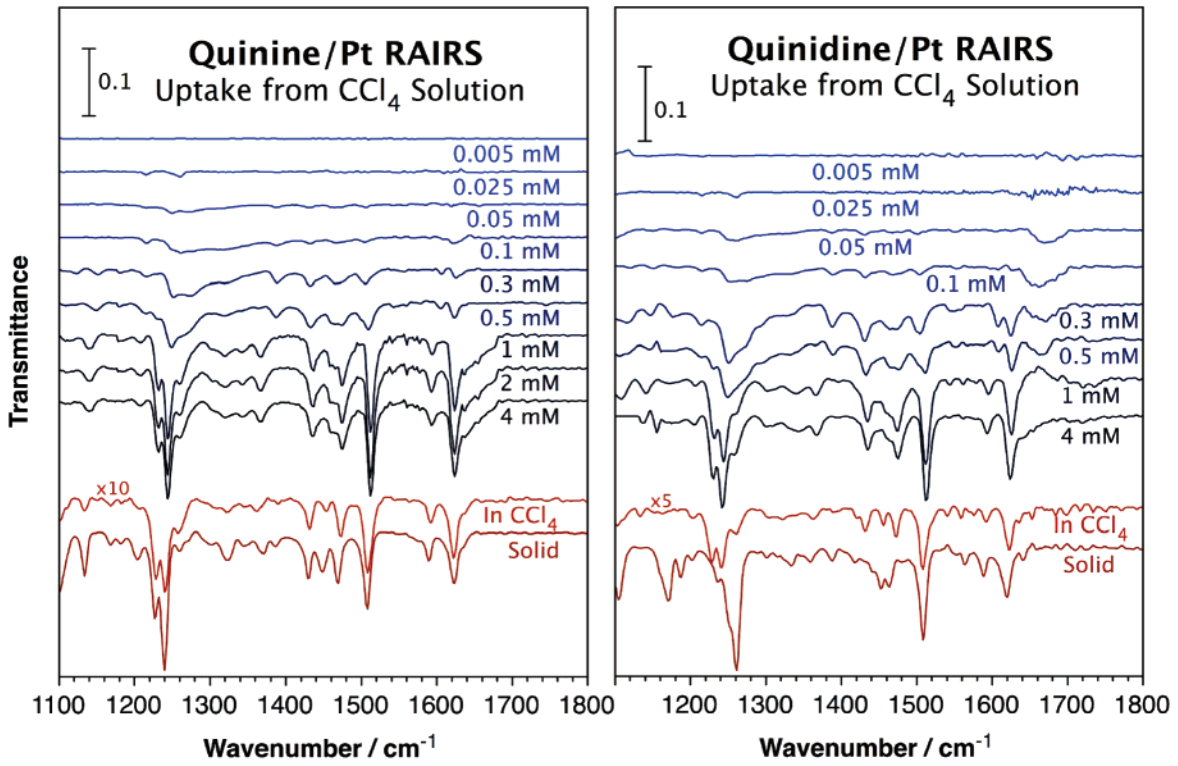

Figure 6. RAIRS for quinine (left panel) and quinoline (right panel) adsorbed on Pt as a function of solution concentration. Similar uptakes are seen with both compounds, with a gradual transition from flat quinoline adsorption to ring tilting indicated by the growth and shift of the C−O stretching vibration peaks of the methoxy group around 1250 cm^{-1}. A unique blue-shift is seen in the frequency of the methoxy modes for the case of solid quinidine, possibly because of crystal field effects.

which point the spectra are dominated by peaks due to the stretching of the C−O bonds in the methoxy group. Those are shifted significantly to the blue because of bonding of the methoxy moiety to the metal via the lone-pair electrons of the

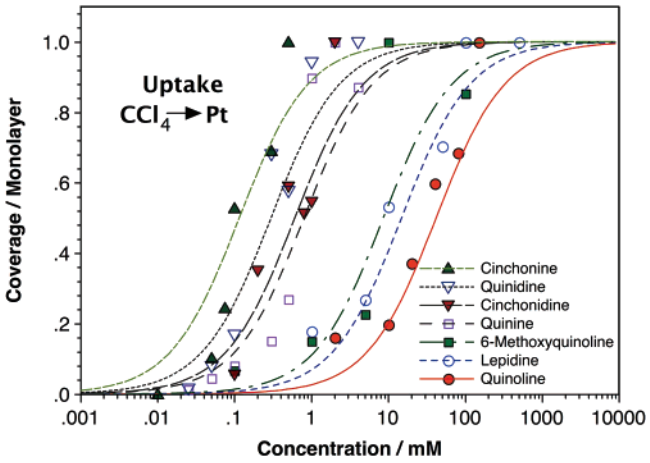

Figure 7. Adsorption uptakes for all the quinoline-derived compounds from CCl_4 solutions onto Pt as a function of concentration, followed using the infrared absorption intensities of key in-plane quinoline ring stretching peaks. The experimental data are shown by the indicated symbols, and fits to simple Langmuir adsorption kinetics by the associated lines. Although the fits are less than ideal, they do provide a semiquantitative way to determine adsorption trends across the family of quinoline derivatives studied here. The equilibrium constants extracted from this analysis are provided in Table 2.

oxygen atom, as corroborated by the detection of the asymmetric methyl deformation mode about 1470 cm^{-1}. The absence of any in-plane ring vibrational modes in the spectra for this concentration range adds to the proposal of flat adsorption. One puzzling difference between the data for quinine and quinidine is that the peaks for the C−O stretching modes in the saturated layer of quinidine on Pt are red-shifted quite far from the values seen in the solid (Figure 6, right frame); this is not the case for quinine (Figure 6, left frame). However, the data clearly show that this anomaly is associated with the solid structure of quinidine, not with its adsorption on the platinum surface; the spectrum for quinidine dissolved in CCl_4 shows the same peak shifts and resembles more closely those of the adsorbed species, and also the IR traces for quinine and quinidine adsorbed on platinum match each other quite closely. We suspect that the dynamic dipoles of the C−O stretching modes may cancel out in solid quinidine because of the pairing of the molecules within each monoclinic unit cell.[48]

The uptakes of all seven quinoline-derived compounds studied here were estimated as functions of their concentrations in solution by averaging the intensities of the most prominent infrared peaks of the tilted adsorbed species. The details of this analysis are provided in Table S1 of the Supporting Information. The data, summarized in Figure 7, indicate different adsorption uptakes for each compound in terms of surface coverages (relative to surface saturation) versus concentration in solution. Langmuir isotherms were fitted to the data to better illustrate those differences, even though they do not represent well the observed adsorption behavior. Indeed, the experimental data display a narrower range of concentrations from the onset of adsorption to saturation than the Langmuir isotherm would predict. Nevertheless, the inflection points of the calculated curves agree reasonably well with the concentrations at which half saturation is observed experimentally, and were used as the parameter of merit to identify adsorption trends. The results of the fits, in the form of inverse equilibrium constants (K_{ads}^{-1}, in units of mM), together with the solubilities of the same compounds in carbon tetrachloride,[49] are reported in Table 2. According to those data, the equilibrium constants follows the sequence quinoline < lepidine <6-methoxyquinoline < quinine < cinchonidine < quinidine < cinchonine.

Table 2. Summary of Adsorption Equilibrium Constants (Estimated from the Data in Figure 7 and Expressed as K_{ads}^{-1}) and Solubilities in CCl_4 for the Quinoline-Derived Compound Studied in This Work

chemical	K_{ads}^{-1}/ mM	solubility in CCl_4/mM	K_{ads}^{-1}/ solubility
quinoline	30	infinite	
lepidine	11	infinite	
6-methoxyquinoline	6.5	infinite	
quinine	0.65	8.63	0.075
cinchonidine	0.5	1.56	0.32
quinidine	0.25	16.3	0.015
cinchonine	0.1	0.30	0.33

4. Discussion

We initiate our discussion with the equilibrium constant ordering for the cinchona alkaloids reported in the last paragraph. In searching for the main factors responsible for the observed sequence, we note that it roughly correlates inversely with the trend observed for solubility, cinchonine < cinchonidine < quinine < quinidine <6-methoxyquinoline ≈ lepidine ≈ quinoline.[49] The argument can easily be made that, for similar compounds, solubility could be the dominating factor determining the adsorption strength reflected by $\Delta H^\circ_{ads,sol}$,[50] because adsorption from solution can be envisioned as an hypothetical two-step process according to the following Hess cycle:

$$\text{cinchona (solution)} = \text{cinchona (solid)} \qquad -\Delta H^\circ_{sol}$$

$$\text{cinchona (solid)} = \text{cinchona (adsorbed)} \qquad \Delta H^{\circ,*}_{ads}$$

$$\text{cinchona (solution)} = \text{cinchona (adsorbed)} \qquad \Delta H^\circ_{ads,sol} = \Delta H^{\circ,*}_{ads} - \Delta H^\circ_{sol}$$

If the adsorption energetics itself, $\Delta H^{\circ,*}_{ads}$, were to be similar for all the compounds being compared, the differences in the overall energetics at the uptake from solution would have to be associated with their solubility. It should be pointed out that the energy differences being considered here are relatively small. Specifically, the solubility enthalpy differences with respect to quinidine can be estimated from the equilibrium constant data in Table 2 (by estimating the appropriate ΔG values and assuming similar entropy values for all compounds) to be 1.6, 7.0, and 10.0 kJ/mol for quinine, cinchonidine, and cinchonine, respectively.

However, the adsorption energetics appears not to be the same. Quinidine in particular displays a much larger K_{ads} than what would be expected from its solubility. One significant clue for why this may be so is the different adsorption geometries that these molecules adopt on the surface at saturation. Recall that, according to our RAIRS data, cinchonidine tilts mainly along its quinoline long axis, whereas cinchonine does it along the short axis. There is a also larger degree of ring distortion in the case of cinchonine, as indicated by the appreciable shifts seen in some key quinoline stretching frequencies. The implica-

(48) Kashino, S.; Haisa, M. *Acta Crystallogr., Sect. C* **1983**, *39*, 310.

(49) Ma, Z.; Zaera, F. *J. Phys. Chem. B* **2005**, *109*, 406.

(50) Adamson, A. W.; Gast, A. P. *Physical Chemistry of Surfaces*, 6th ed.; Wiley-Interscience: New York, 1997.

tion is that cinchonine adsorption at high coverages relies heavily on a σ bond between the quinoline nitrogen lone electron pair and the surface metal atom(s). The reorientation of the cinchonidine, in contrast, may be driven predominantly by intermolecular interactions ($\pi-\pi$ stacking). Moreover, although similar adsorption trends are observed for quinine versus quinidine as a function of surface coverage (that is, as their concentration in solution is increased), in both those cases the ring tilting occurs progressively rather that abruptly as with cinchonidine and cinchonine. This appears to be because of an additional interaction between the oxygen atom in the methoxy group of the quinoline and the surface, even if that interaction appears to be superseded by other forces at higher concentrations. All these different adsorption modes are expected to display different adsorption energetics.

Surprisingly, the K_{ads} values in Table 2 do not entirely match the ability of one cinchona to displace another in a competitive adsorption environment either. This was determined in previous experiments to follow the sequence quinine $\sim$ quinidine > cinchonidine > cinchonine >6-methoxyquinoline > lepidine > quinoline.[16] It appears that, again, competitive adsorption may be affected by both the absolute adsorption strength of the molecule on the surface and its solubility. A balance between those two driving forces can be estimated by expressing the adsorption equilibrium constants not in absolute terms but relative to the appropriate solubilities instead,[51] as suggested by the Hess cycle above. When viewed in that light, the relative adsorption equilibrium constants for the cinchona alkaloids do follow the same trend obtained in competitive adsorption experiments (Table 2). This balance of forces may also explain some inconsistencies in previous reports on the adsorption and catalytic behavior of different cinchona alkaloids. In particular, it may seem difficult to reconcile the fact that cinchonine is easily displaced from the platinum surface by cinchonidine, quinine, or quinidine even though, according to the results reported here, the former displays a higher absolute adsorption equilibrium constant than the others. Cinchonine does bond more strongly to the surface because of the interaction of its nitrogen lone electron pair with the metal (as indicated above), but its displacement is facilitated by the higher solubilities of the other cinchona in the CCl_4 solvent. On the other hand, since cinchonidine, quinidine and quinine all display comparable equilibrium constants, their ability to displace one another is dominated by their differences in solubility.

One of the key contributions of the present work to the understanding of cinchona adsorption is the identification of some difference in the uptake behavior on the surface among closely related cinchona alkaloids. The interest in understanding those differences is driven by the fact that the cinchona molecules, although very similar in structure, behave quite differently in catalytic applications. For instance, although cinchonine and cinchonidine are near enantiomers and promote the production of opposite enantiomers during the catalytic hydrogenation of α-keto esters, they do this to significantly different degrees.[9,52−54] An extreme manifestation of such behavior is seen in the nonlinear effects observed when mixtures of cinchonine + cinchonidine or of quinine + quinidine are used as chiral modifiers: the resulting enantioselectivity does not add up to the combination of those of the elements in these chiral mixtures, but rather to that of only one particular modifier.[8,10,12−14] This has been traced back to a competitive adsorption of modifiers on the surface, which typically leads to the preferential adsorption of one of the cinchona compounds.[11,15,16] The question still remains on what are the fundamental physical properties that control the adsorption strengths of these closely related molecules.

Our study sheds some light on this question. Specifically, our in-situ infrared characterization allowed us to identify different adsorption geometries for each of the cinchona alkaloids reported here. For instance, although both cinchonidine and cinchonine undergo a molecular reorientation from flat quinoline adsorption at low concentrations to a more tilted configuration in more concentrated solutions, cinchonidine tilts mainly along its quinoline long axis whereas cinchonine does it along the short axis instead. There is a larger degree of ring distortion in the case of cinchonine as well, as indicated by the appreciable shifts seen in some key quinoline stretching frequencies. The implication is that cinchonine adsorption at high coverages relies heavily on a σ bond between the quinoline nitrogen lone electron pair and the surface metal atom(s). The reorientation of the cinchonidine may be driven predominantly by intermolecular interactions ($\pi-\pi$ stacking) instead.

Finally, it must be said that the Hess cycle used in this discussion fails to take into account the effect of the solvent on the energetics of the adsorbed species directly. Put another way, the heat of adsorption associated with the second step there, $\Delta H^{\circ,*}_{ads}$, is not the same as the heat of adsorption typically estimated in gas-phase experiments, ΔH°_{ads}. This is an important distinction, because the data in Figure 2 clearly indicates that the adsorbates bond significantly differently in the presence versus in the absence of the solvent. It also raises some questions on the relevance of the studies reported for these and other related molecules under vacuum conditions[55−60] to the understanding of chiral modification during catalytic hydrogenation processes, which take place in the presence of liquid solutions in contact with the solid catalyst. In fact, our previous work has indicated that some of the quinoline compounds undergo dehydrogenation in vacuum around room temperature,[32] and therefore lose their ability to reversibly adsorb on the surface of metals; this is believed to be needed for the chiral modification effect in catalysis.

5. Conclusions

The adsorption of a number of quinoline derivatives from carbon tetrachloride solutions onto platinum surfaces was characterized in situ by RAIRS. It was found that in all cases the spectra of the adsorbed species were significantly different

(51) Hansen, R. S.; Craig, R. P. *J. Phys. Chem.* **1954**, *58*, 211.
(52) Blaser, H. U.; Jalett, H. P.; Monti, D. M.; Baiker, A.; Wehrli, J. T. *Stud. Surf. Sci. Catal.* **1991**, *67*, 147.
(53) Bartók, M.; Sutyinszki, M.; Balázsik, K.; Szöllodblacsi, G. *Catal. Lett.* **2005**, *100*, 161.
(54) Sonderegger, O. J.; Ho, G. M.-W.; Bürgi, T.; Baiker, A. *J. Mol. Catal. A: Chem.* **2005**, *229*, 19.
(55) Carley, A. F.; Rajumon, M. K.; Roberts, M. W.; Wells, P. B. *J. Chem. Soc., Faraday Trans.* **1995**, *91*, 2167.
(56) Evans, T.; Woodhead, A. P.; Gutiérrez-Sosa, A.; Thornton, G.; Hall, T. J.; Davis, A. A.; Young, N. A.; Wells, P. B.; Oldman, R. J.; Plashkevych, O.; Vahtras, O.; Ågren, H.; Carravetta, V. *Surf. Sci.* **1999**, *436*, L691.
(57) Stephenson, M. J.; Lambert, R. M. *J. Phys. Chem. B* **2001**, *105*, 12832.
(58) Bonello, J. M.; Lambert, R. M. *Surf. Sci.* **2002**, *498*, 212.
(59) Bonello, J. M.; Lindsay, R.; Santra, A. K.; Lambert, R. M. *J. Phys. Chem. B* **2002**, *106*, 2672.
(60) Wahl, M.; Von Arx, M.; Jung, T. A.; Balker, A. *J. Phys. Chem. B* **2006**, *110*, 21777.

than those of the pure substances in that they display varying relative peak intensities and easily measurable peak shifts. On the other hand, those changes were only observable in the case of adsorption from solution; no equivalent RAIRS traces were obtained for the molecules in solution or adsorbed on platinum under vacuum conditions.

A comparative study was performed with three basic quinoline-based compounds, namely, quinoline, lepidine, and 6-methoxyquinoline, and four closely related cinchona alkaloids, cinchonidine, cinchonine, quinine, and quinidine. The uptakes of the reference compounds were found to all follow similar behavior, with no fundamental changes as a function of concentration in solution other than an increase in total surface coverage. On the other hand, more complex behavior was observed with the cinchona. Those all adsorb with their quinoline ring flat on the surface at low concentrations and then tilt abruptly upon increasing coverages, but the switchover takes place at significantly different solution concentrations in each case. In addition, each compound displays some unique behavior. The quinoline ring in cinchonidine tilts along its long axis, presumably to optimize $\pi-\pi$ intermolecular interactions. In contrast, cinchonine tilts along the short axis, and preserves a stronger interaction of the nitrogen atom in the quinoline moiety with the surface. Both quinine and quinidine undergo a more gradual surface rearrangement, involving some additional bonding through the methoxy oxygen atom at intermediate concentrations. These adsorption differences, together with differences in solubility, explain the relative adsorption strengths of the four cinchona alkaloids studied here, and also some apparent contradictions in behavior reported in the literature in terms of their effectiveness as chiral catalysis promoters.

Acknowledgment. Financial support for this work was provided by the U.S. Department of Energy.

Supporting Information Available: Additional in situ RAIRS data for the uptake of lepidine and 6-methoxyquinoline on Pt as a function of concentration in solution and for the estimation of errors related to the equilibrium constants reported in Table 2 and Figure 7. This material is available free of charge via the Internet at http://pubs.acs.org.

JA076011A